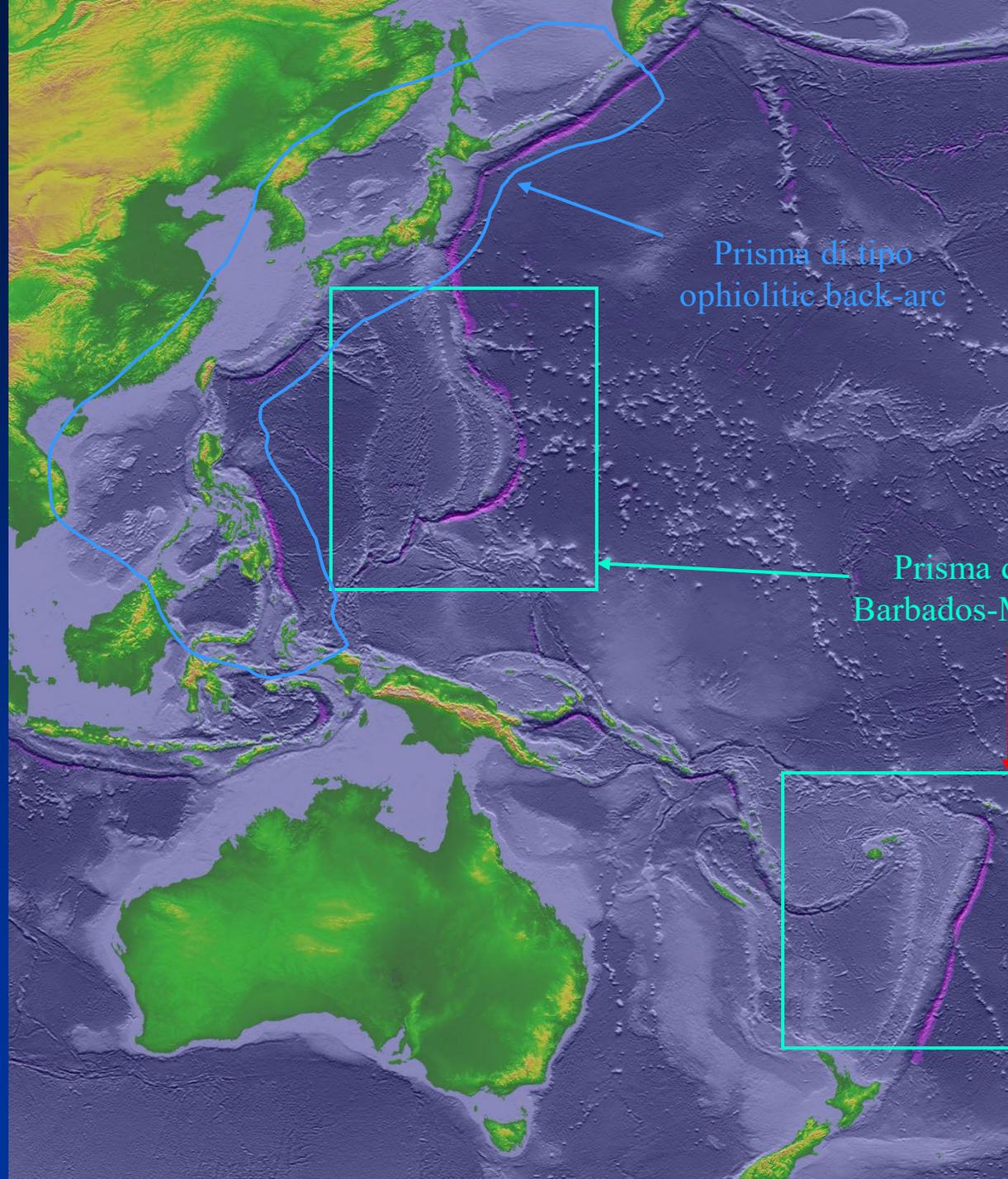Shaded reliefs e batimetria da NOAA National Centers for Environmental Information (NCEI)

Shaded reliefs e batimetria da NOAA National Centers for Environmental Information (NCEI)

Prisma di tipo ophiolitic back-arc

Prisma di tipo Barbados-Marianne

Shaded reliefs e batimetria da NOAA National Centers for Environmental Information (NCEI)

Zona di subduzione delle
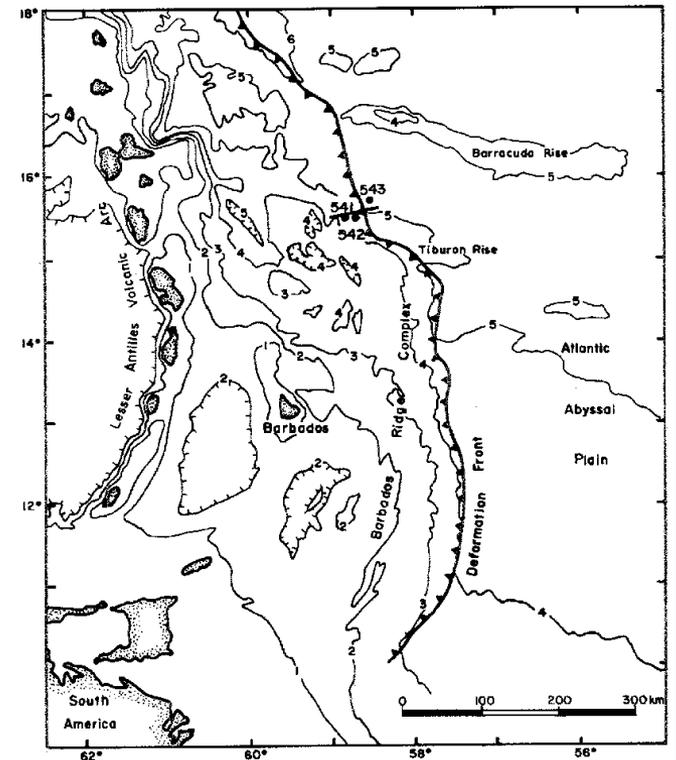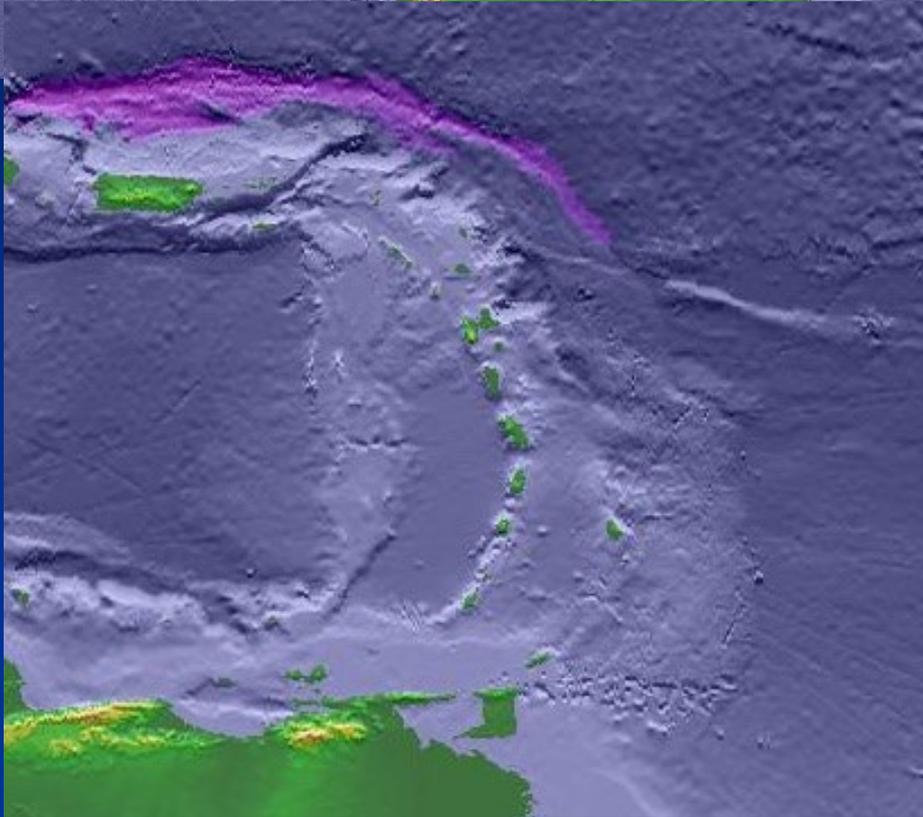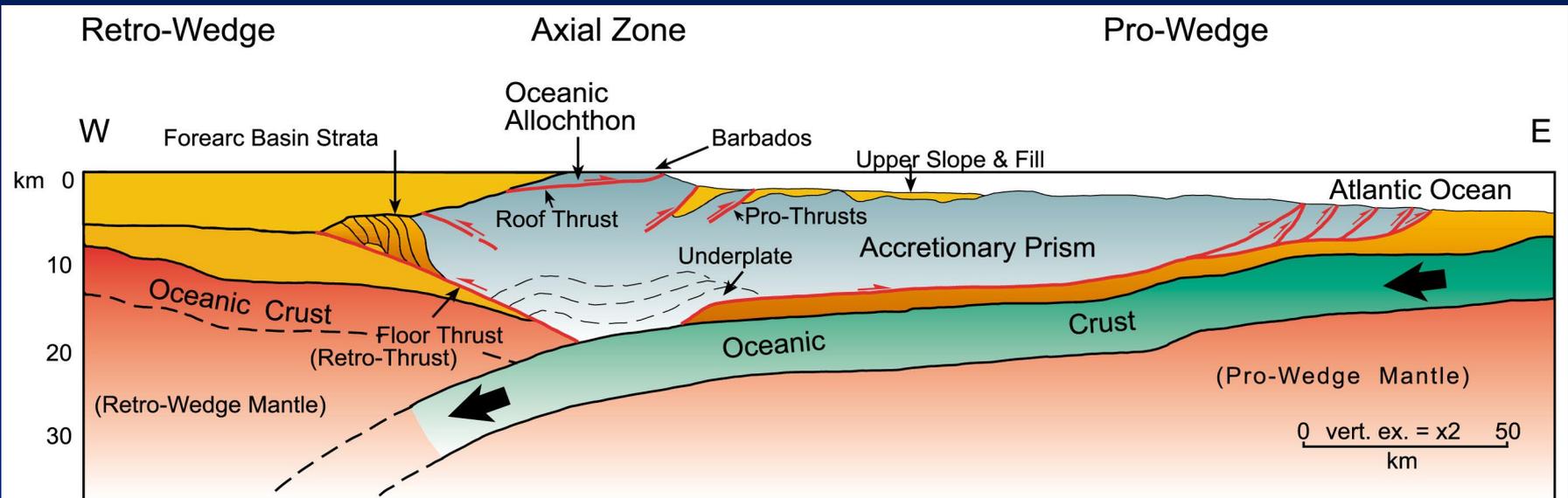Piccole Antille - Barbados

Figure 2. Location of Leg 78A drilling sites near deformation front of Barbados Ridge complex. Bathymetric contours in kilometers.

Moore and Lundberg, 1986

Retro-Wedge   Axial Zone   Pro-Wedge

Oceanic Allochthon

W   Forearc Basin Strata   Barbados   Upper Slope & Fill   E

km 0   Atlantic Ocean

Roof Thrust   Pro-Thrusts

Accretionary Prism

10   Underplate

Oceanic Crust

Floor Thrust (Retro-Thrust)   Oceanic   Crust

20   (Pro-Wedge Mantle)

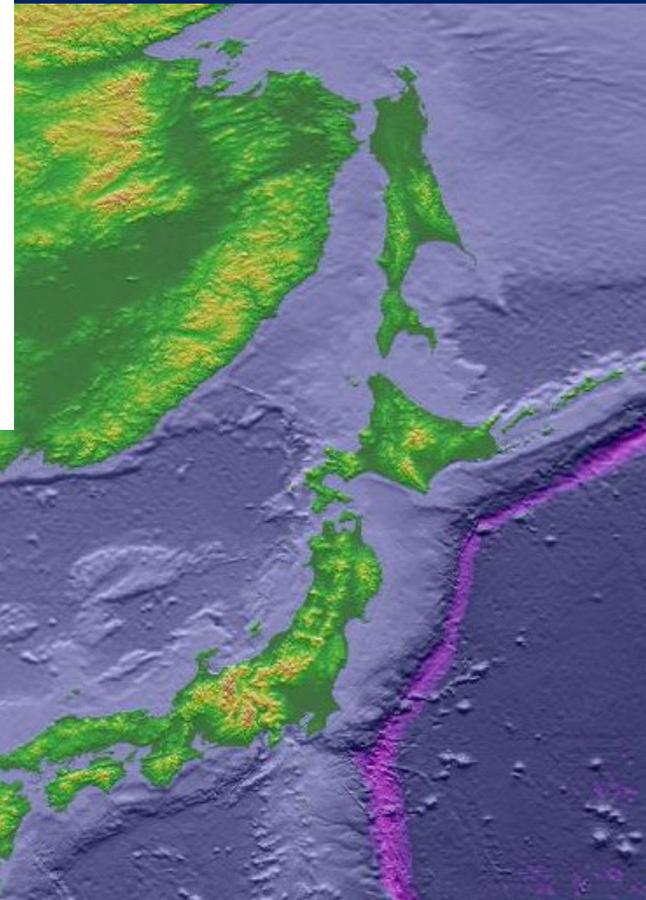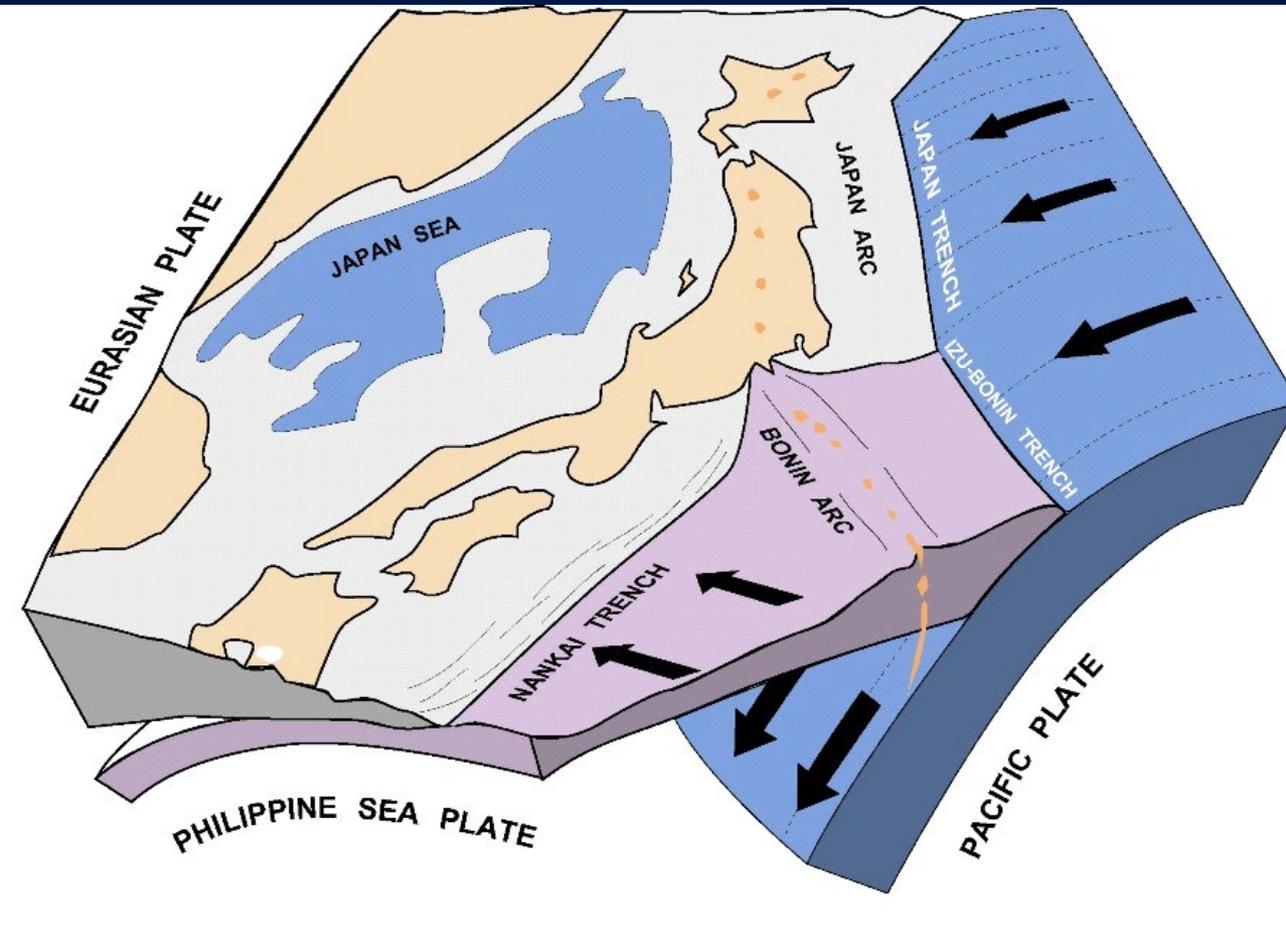(Retro-Wedge Mantle)

0   vert. ex. = x2   50

30   km

(From Torrini & Speed, 1989)

Shaded reliefs e batimetria da NOAA National Centers for Environmental Information (NCEI)
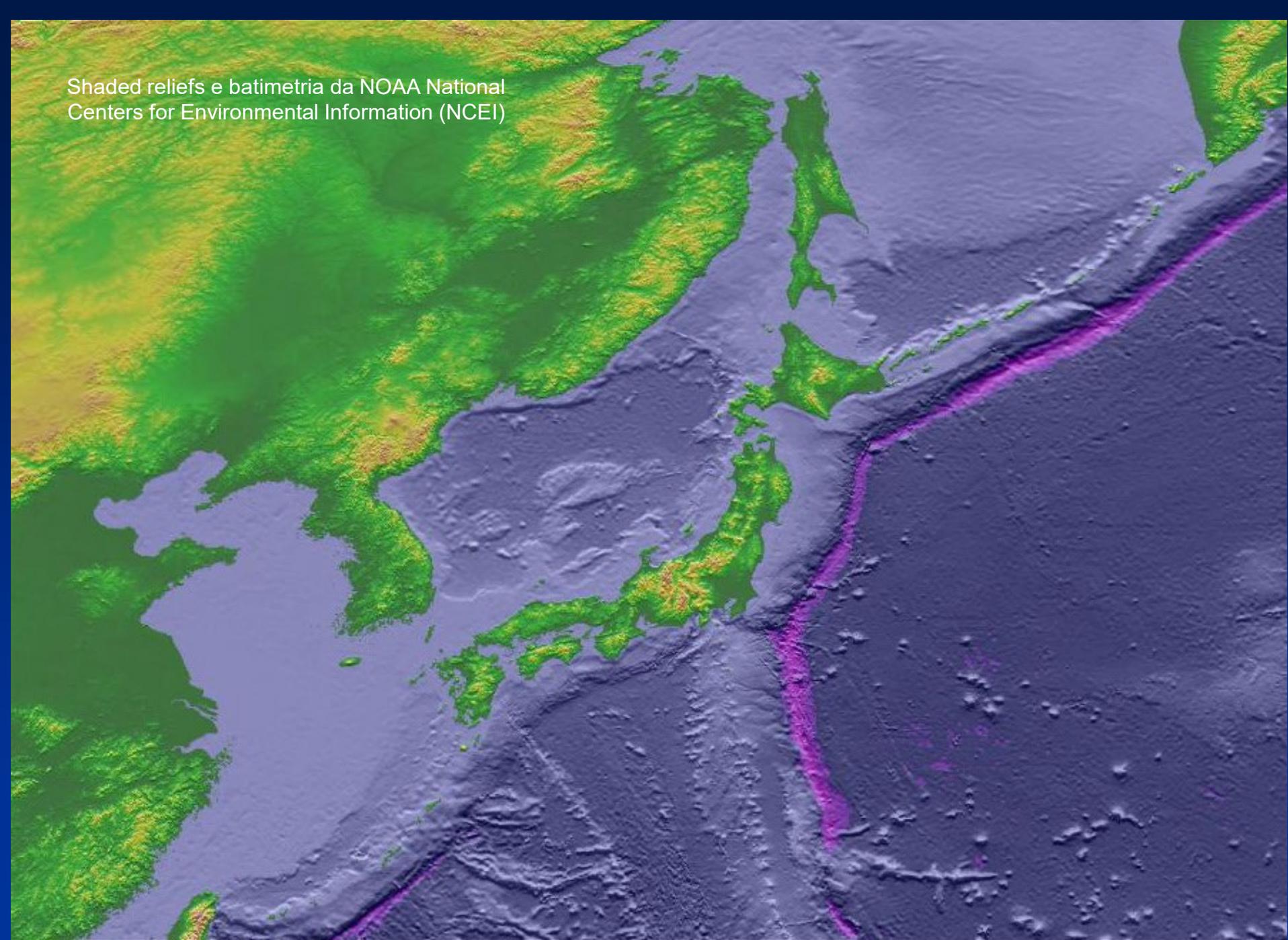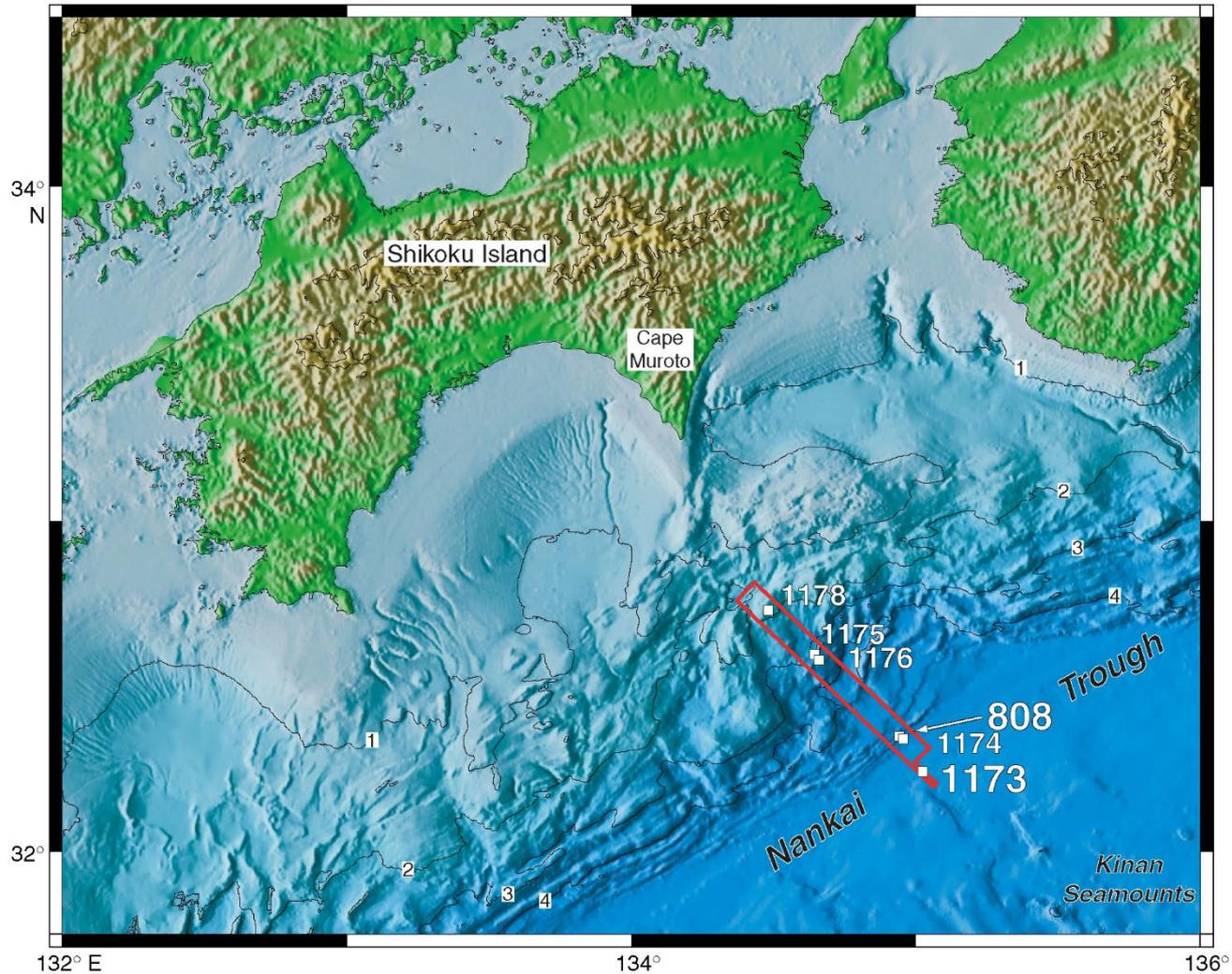
Laurent Jolivet, Sorbonne Université, CNRS-INSU

Shaded reliefs e batimetria da NOAA National Centers for Environmental Information (NCEI)

Figure F1. Map showing locations of Leg 190 and 196 sites. The red box outlines the location of the three-dimensional seismic survey. Yellow numbers indicate sites revisited during Leg 196. Depth contours are in kilometers.

Shipboard Scientific Party, 2002. Chapter 1, Summary. In Proceedings of the ODP, Initial Reports, Leg 196
http://www-odp.tamu.edu/publications/196_IR/chap_01/chap_01.htm

Giappone (Nankai Trench)

Chapter 1, Figure F8. Composite seismic section through Leg 196 drill sites. See map (upper right) for location and geometry of the composite construction. These data were obtained as part of a three-dimensional (3-D) seismic reflection volume acquired during a 1999 *Ewing* cruise. The top section is a two-dimensional prestack depth-migrated version of a section from the 3-D data volume. The bottom section shows the same data converted to time. This version of the data is from Hills et al. (2001). CMP = common midpoint, VE = vertical exaggeration.

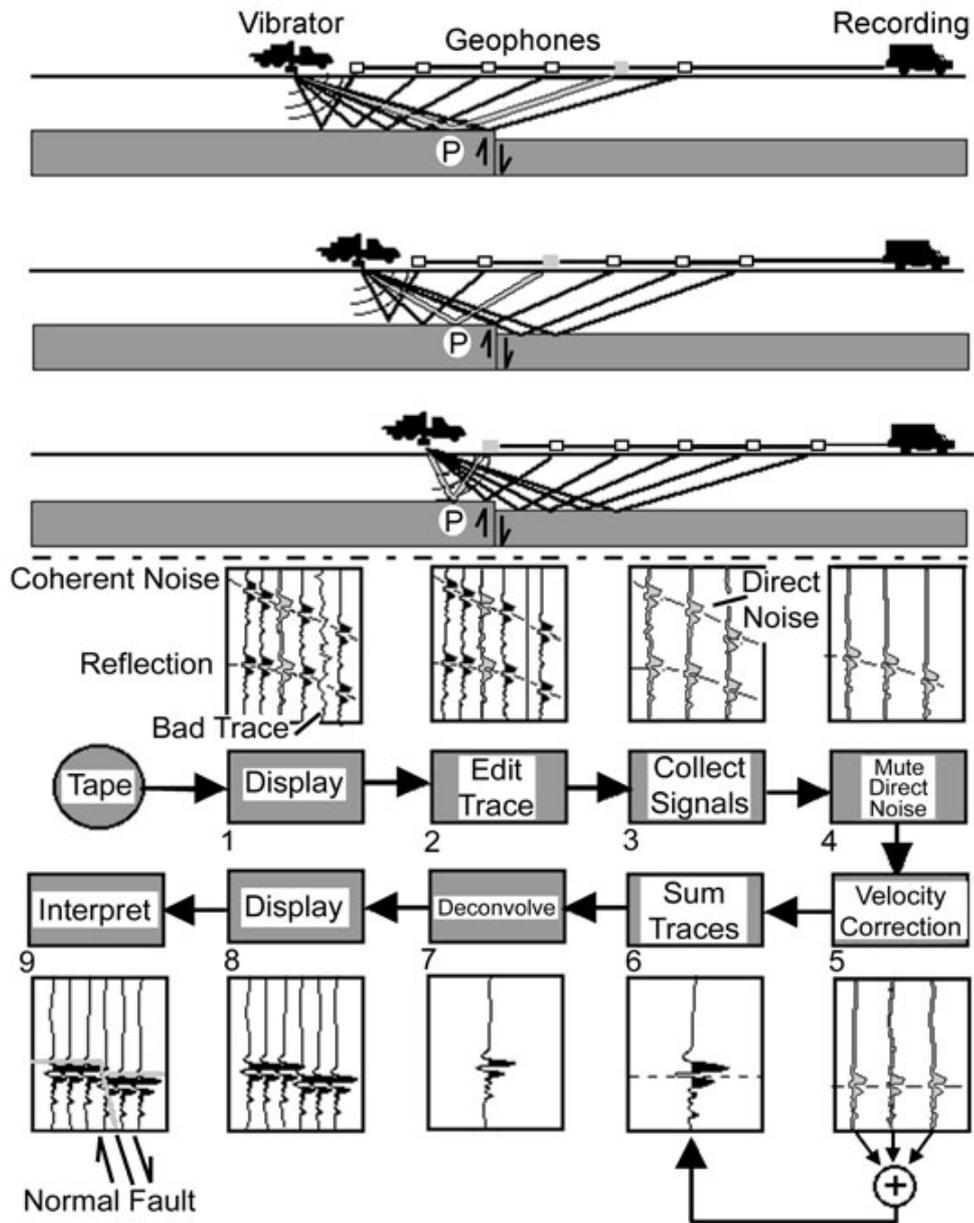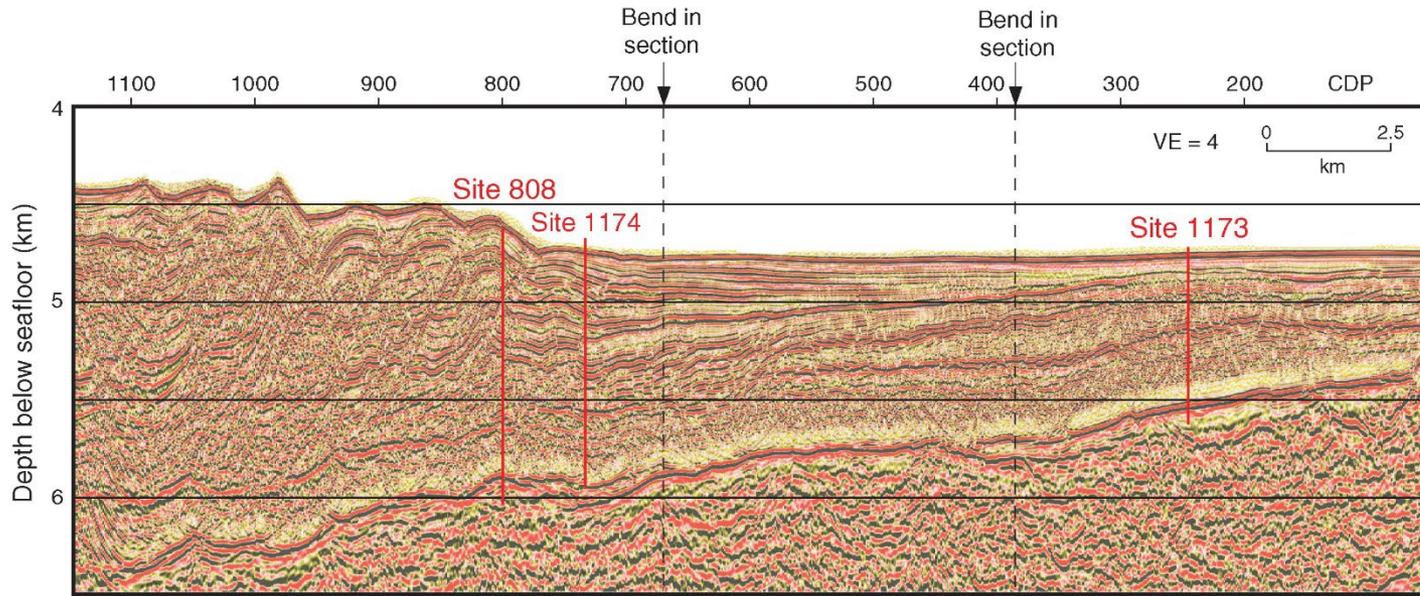Da van der Pluim & Marshak, 2004
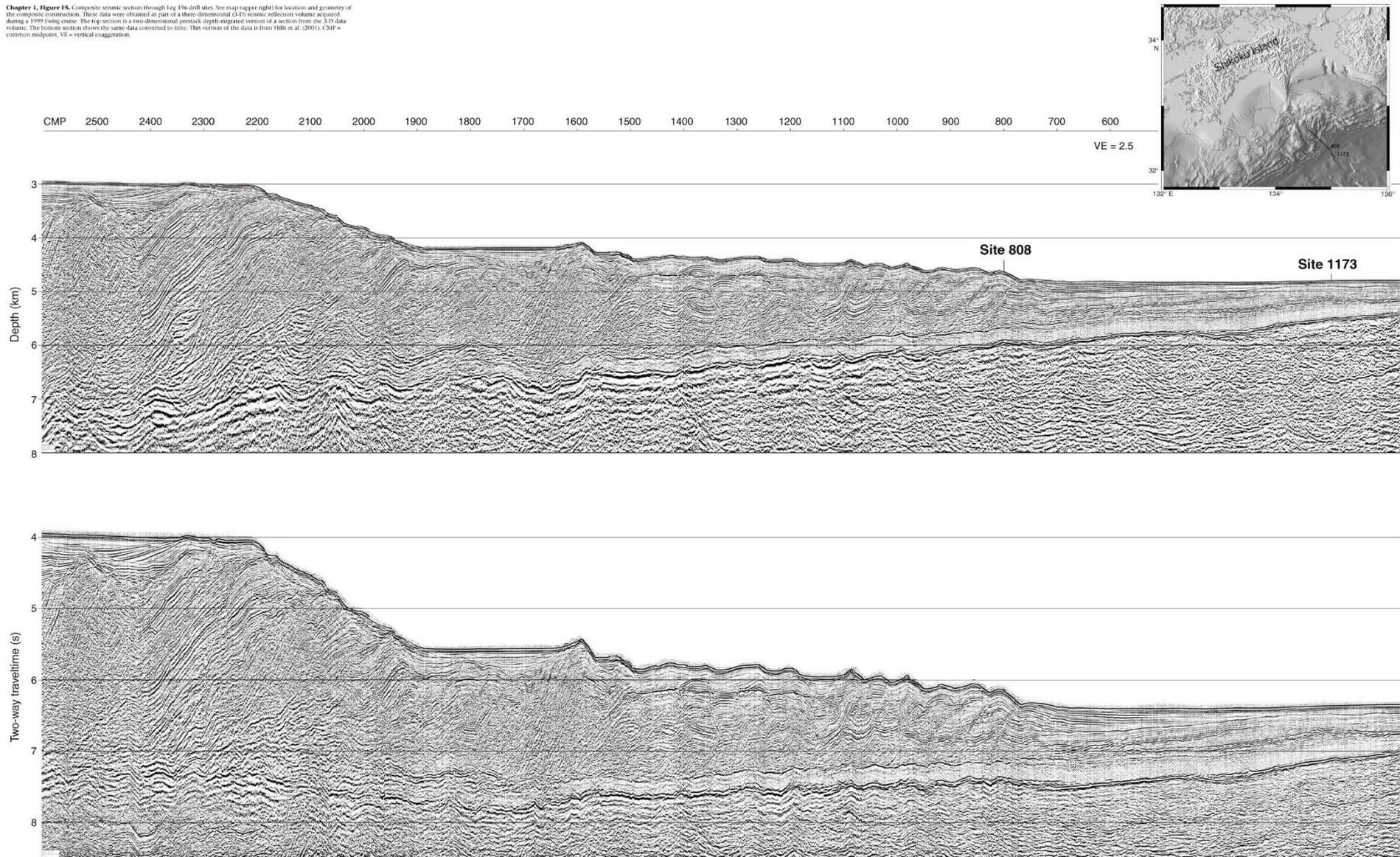
Figure F4. Seismic depth section across Sites 1173, 1174, and 808 (Hills et al., 2001). The section is composed of a northwest-trending segment of seismic line 215 through Site 1173, with a diagonal transition to line 281 that passes near Sites 1174 and 808. CDP = common depth point, VE = vertical exaggeration.
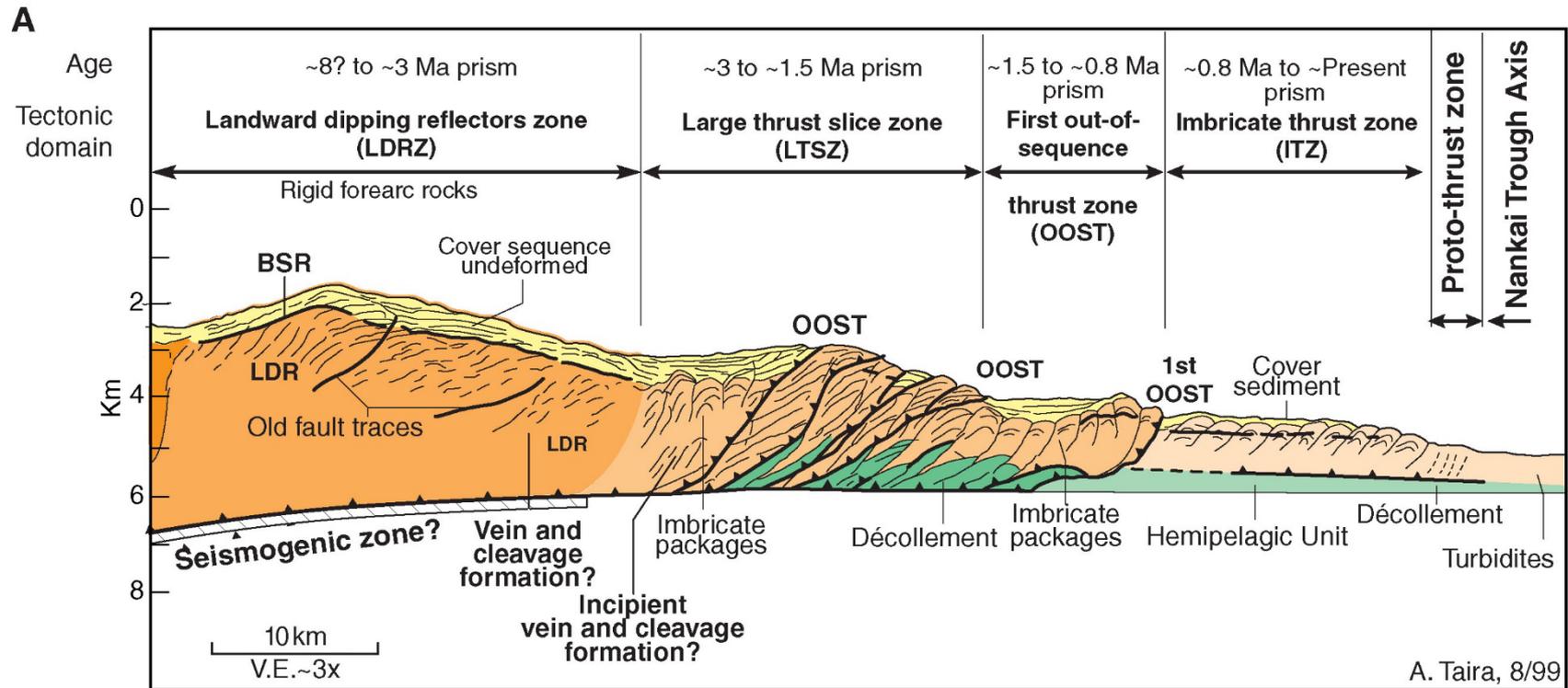
koku Basin to the imbricate thrust zone.
liagonal transition to line 281 that passes

Shipboard Scientific Party, 2002. Chapter 1, Summary. In Proceedings of the ODP, Initial Reports, Leg 196
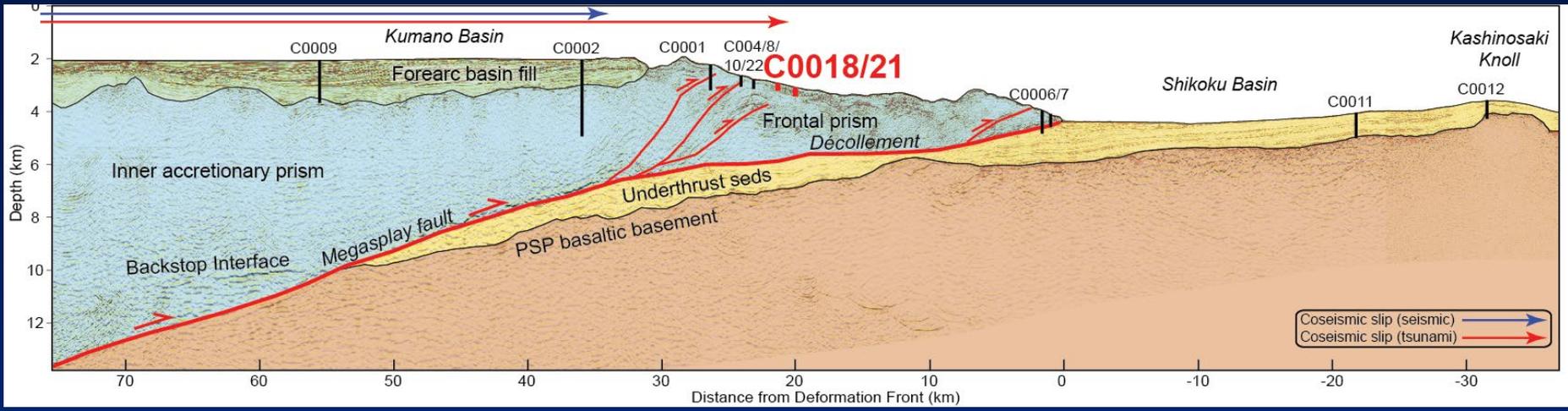http://www-odp.tamu.edu/publications/196_IR/chap_01/chap_01.htm
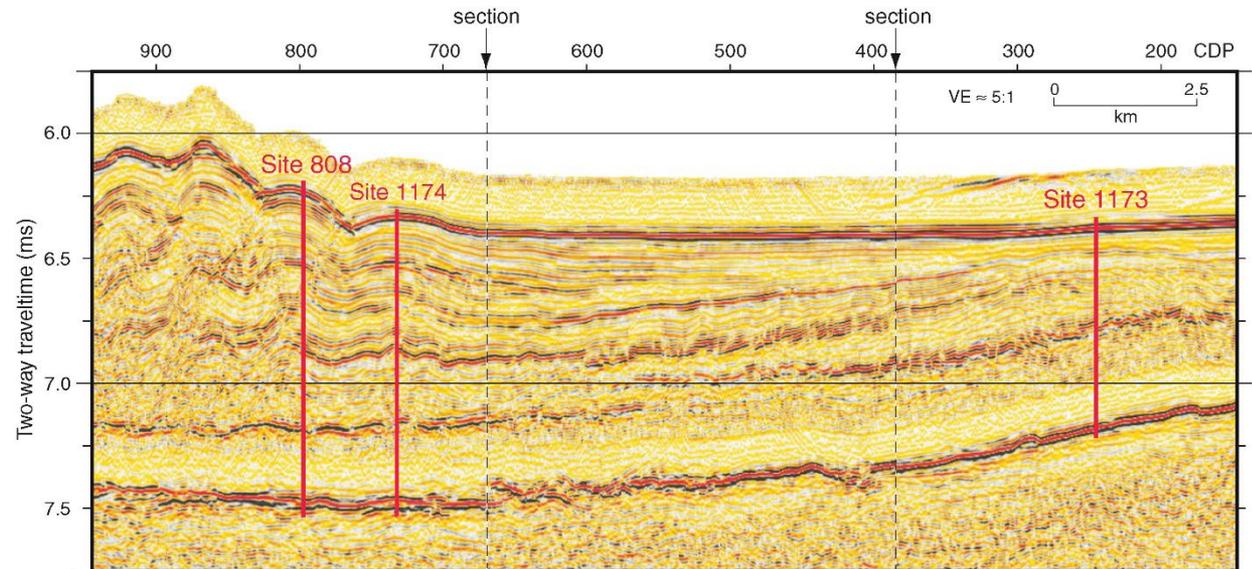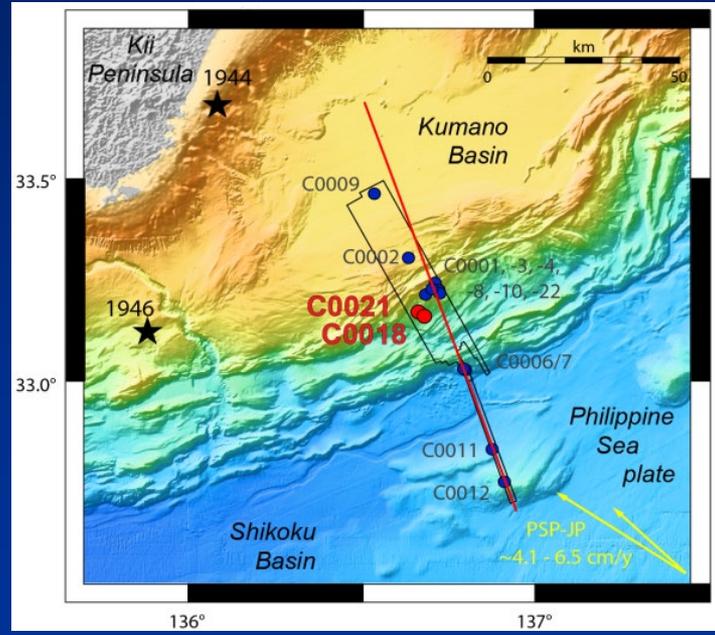
Giappone (Nankai Trench)

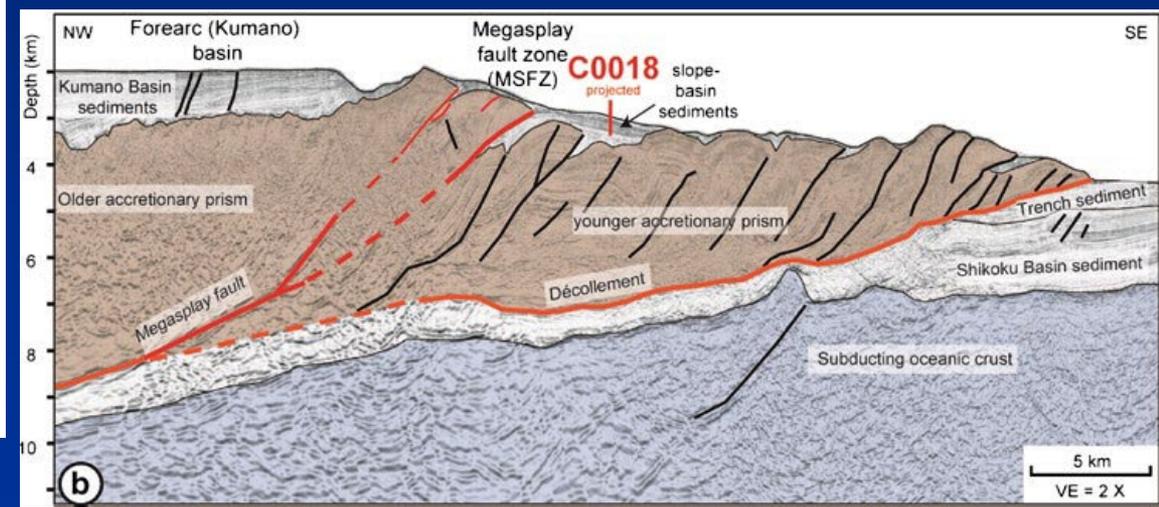Moore, Taira, Baldauf & Klaus, 2000, ODP Scientific Prospectus Leg 190
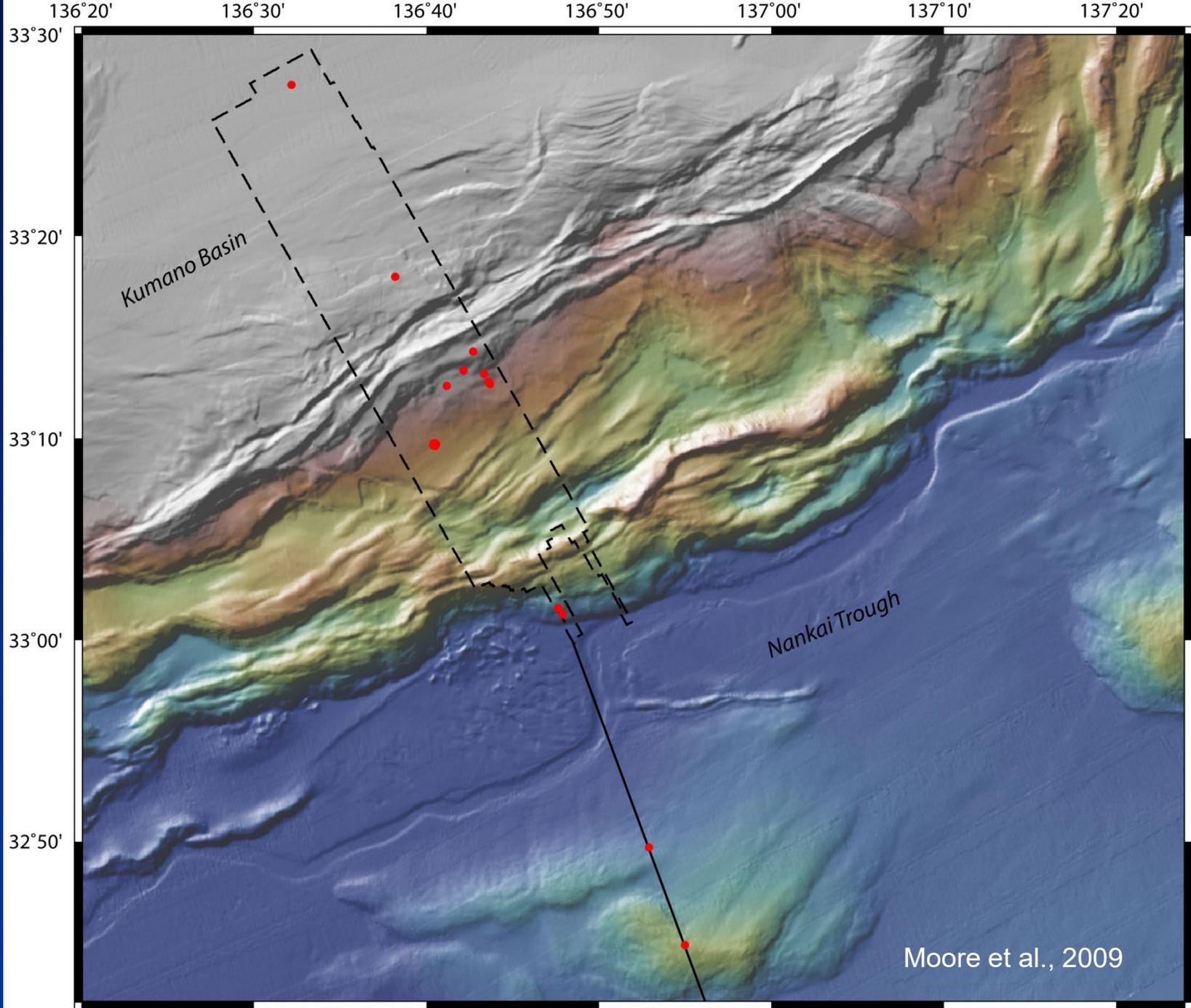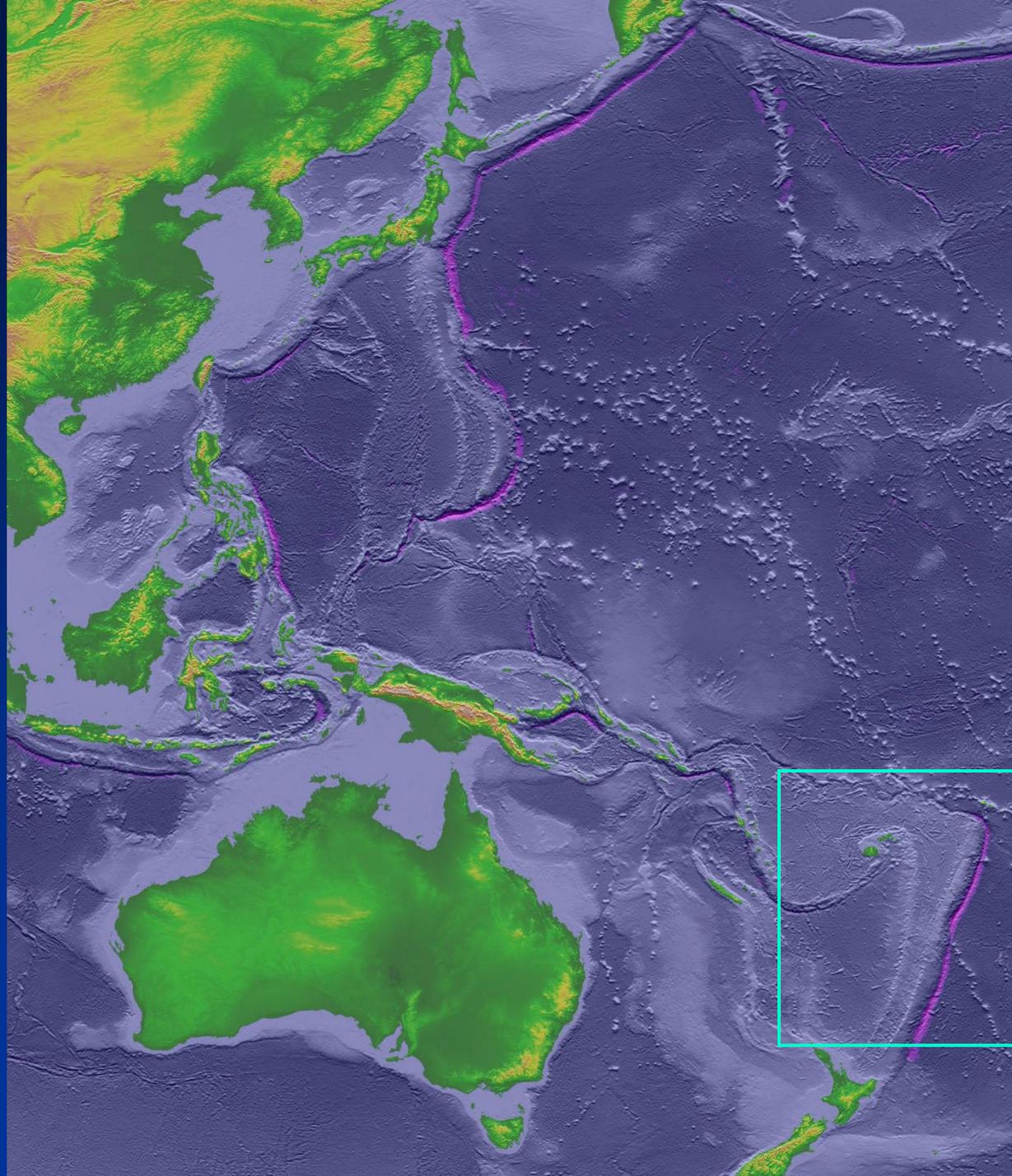http://www-odp.tamu.edu/publications/prosp/190_prs/190toc.html

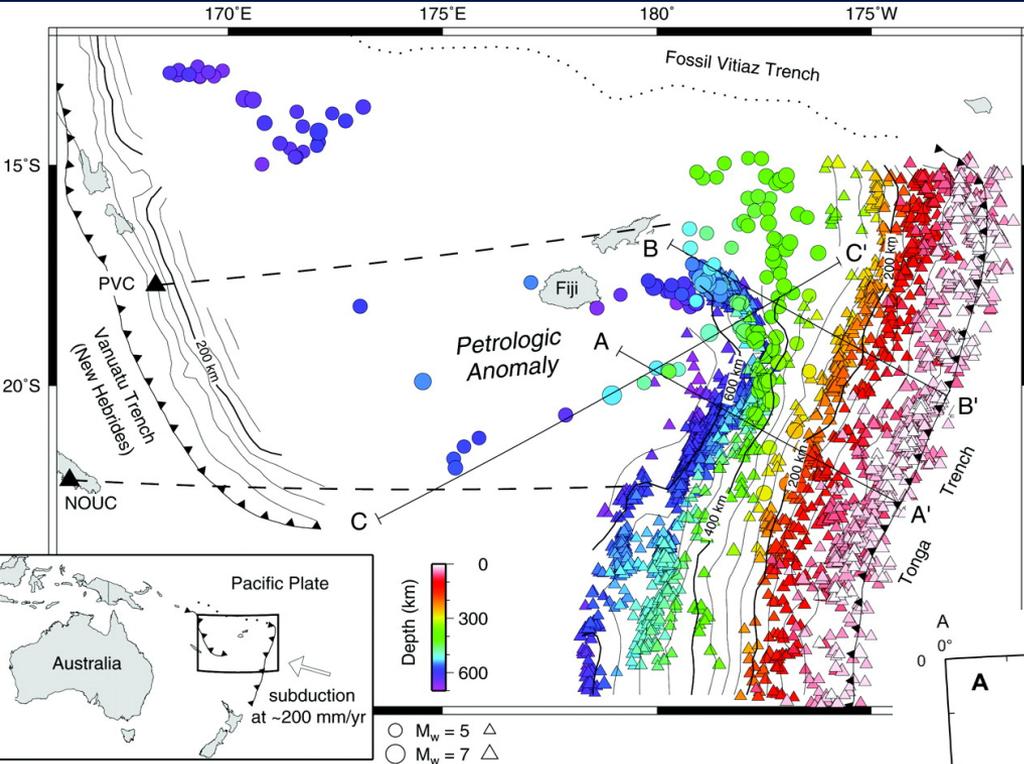Moore et al., 2014

Moore et al., 2014

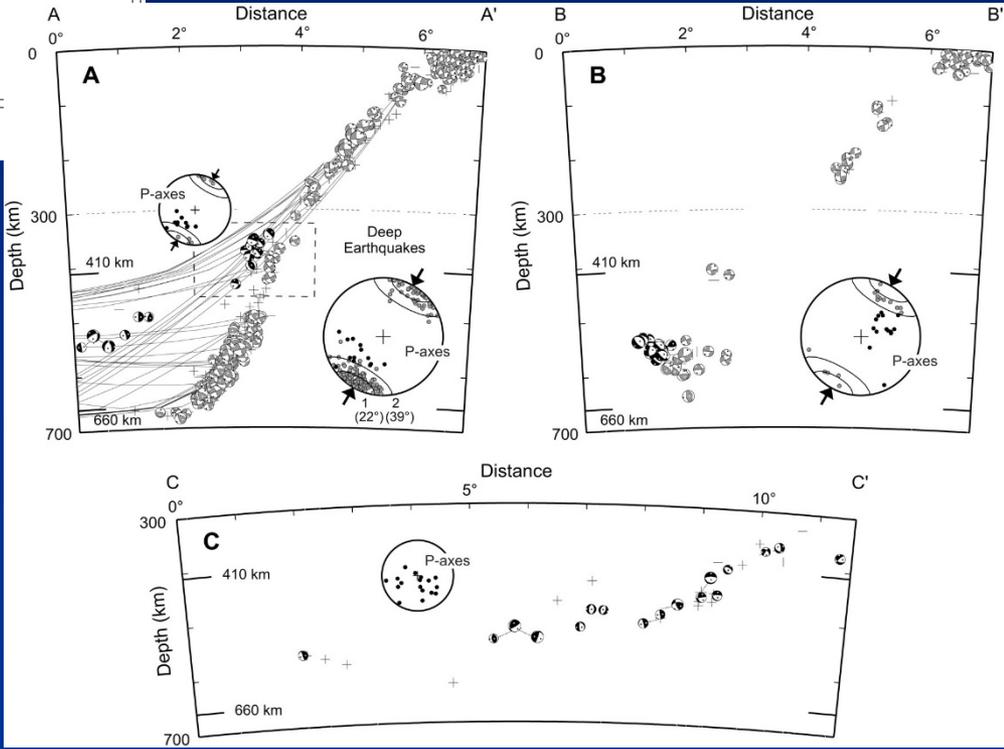Strasser et al., 2012

Moore et al., 2009

Shaded reliefs e batimetria da NOAA National Centers for Environmental Information (NCEI)
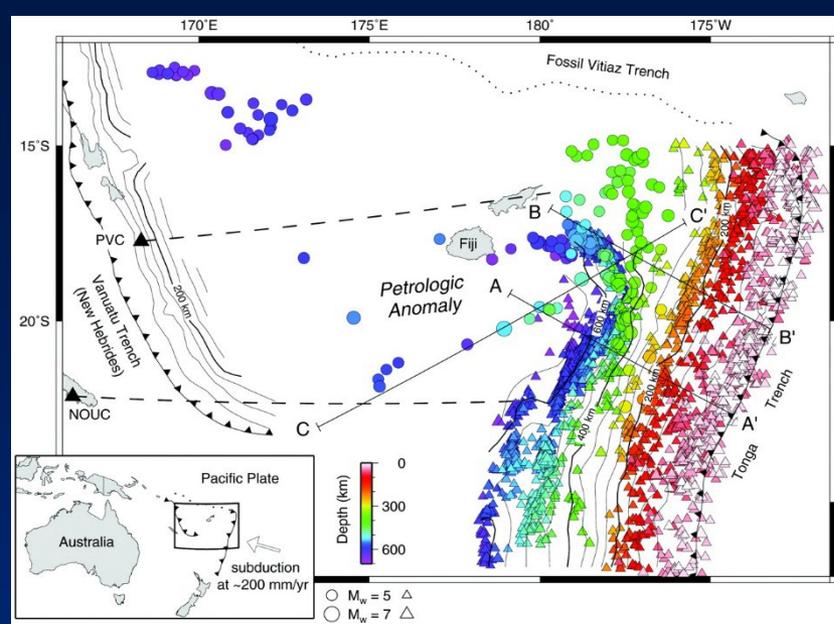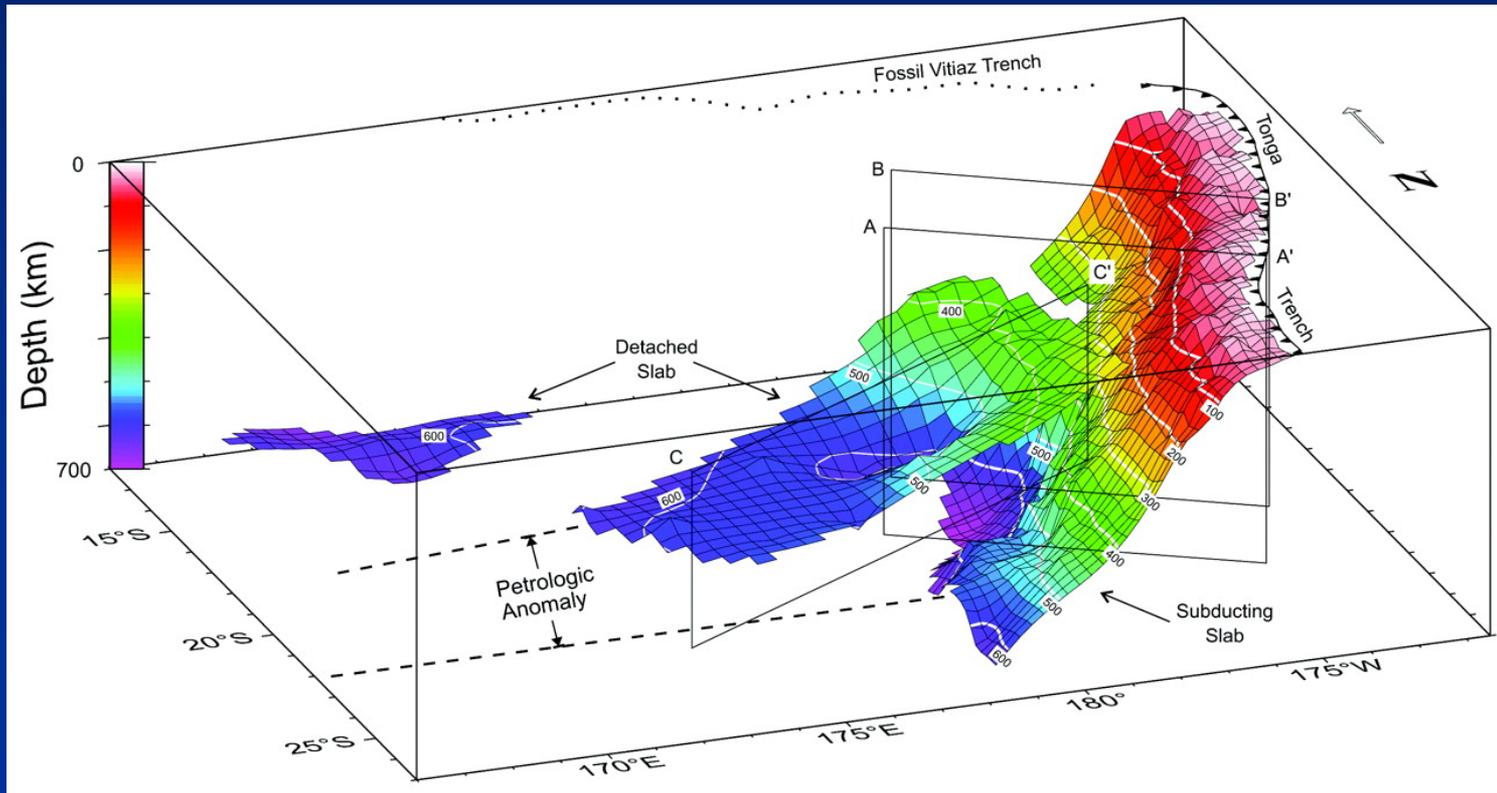
Mappa e tre sezioni crostali-mantelliche mostranti la profondità degli ipocentri dei terremoti a magnitudo ≥ 5 occorsi tra il 1964 e il 1999 nelle Tonga Fiji.

Da Cheng & Brudzinski, 2001

Ricostruzione 3D della sismicità sotto alla fossa-retroarco di Tonga

Da Cheng & Brudzinski, 2001

Prismi di accrezione: cordillera-andino

Prisma di tipo
Barbados-Marianne

Prisma di tipo
cordillera-andino

Shaded reliefs e
batimetria da NOAA
National Centers for
Environmental
Information (NCEI)

Shaded reliefs e batimetria da NOAA National Centers for Environmental Information (NCEI)

DEPTH SECTION LAMONT-DOHERTY LINE C130 CDP'S 3000-5500
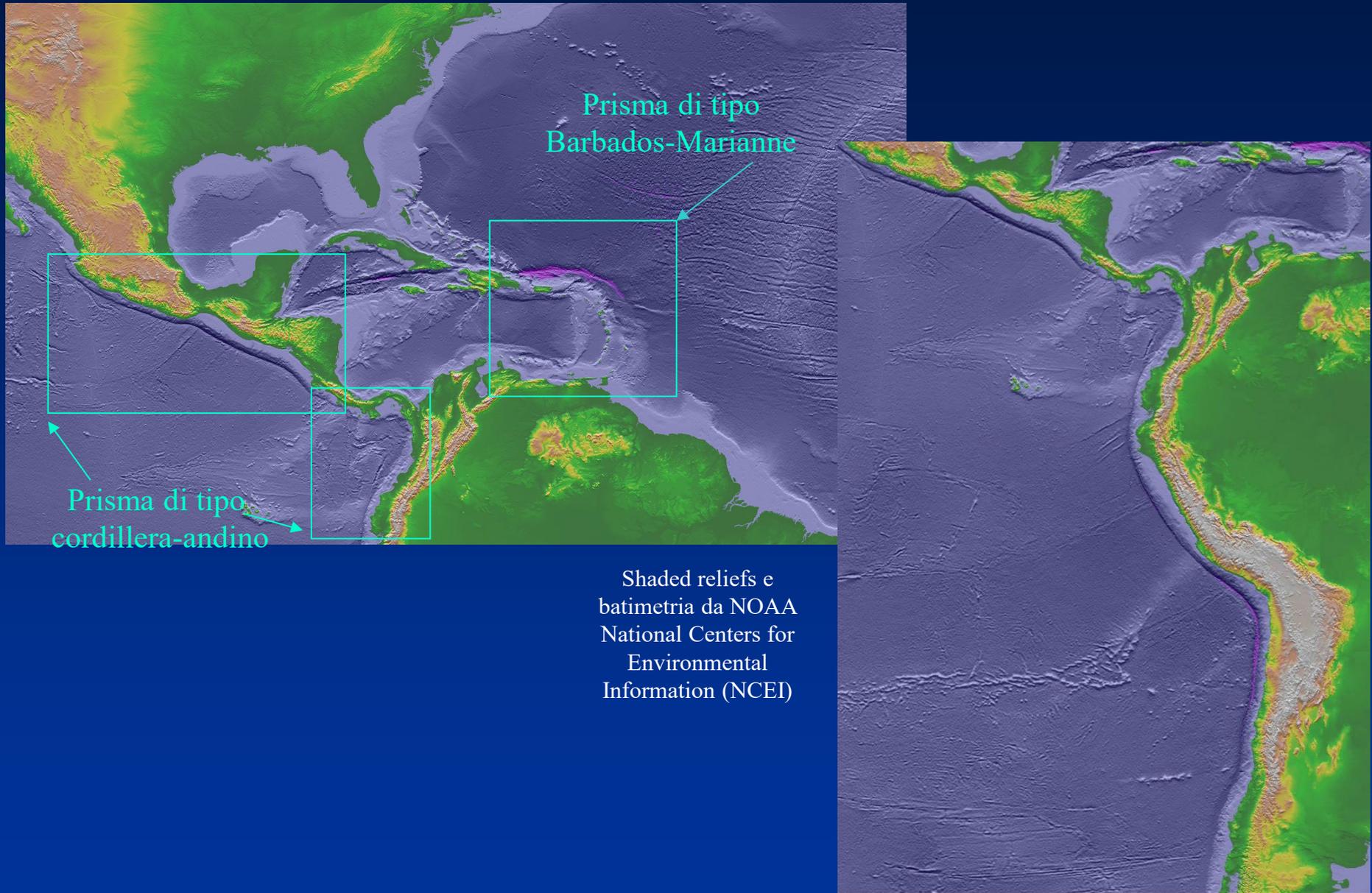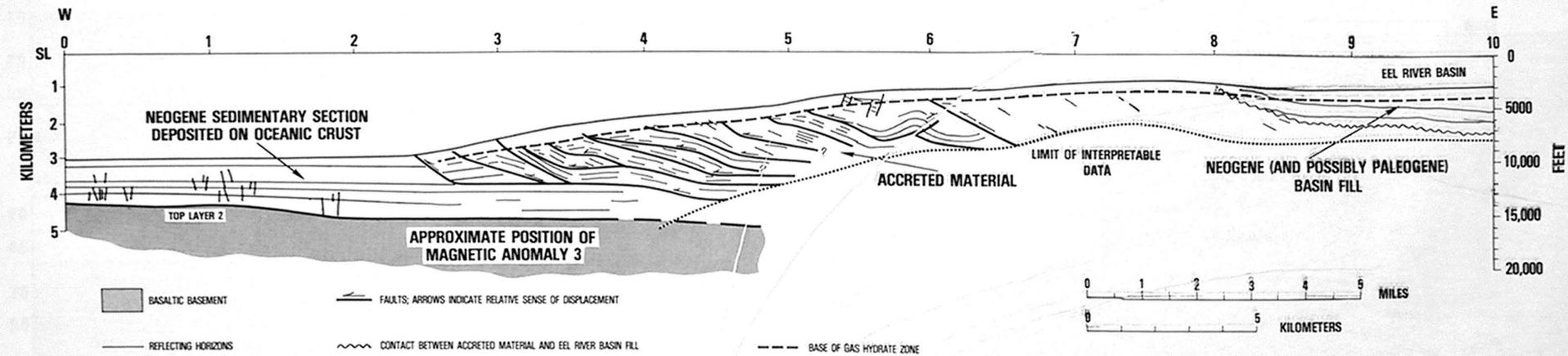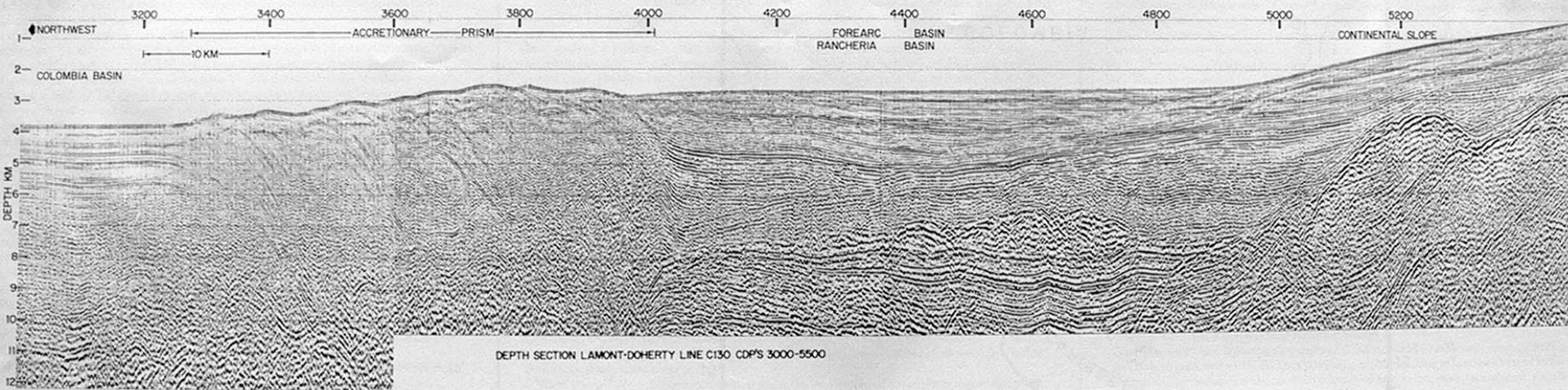
STRUCTURE OF SUBDUCTION COMPLEX,
OFFSHORE NORTHERN CALIFORNIA

FIGURE 5

GEOLOGICAL CROSS SECTION;
NO VERTICAL EXAGGERATION

Tipo cordillera o andino

Da Bally (ed.), 1985
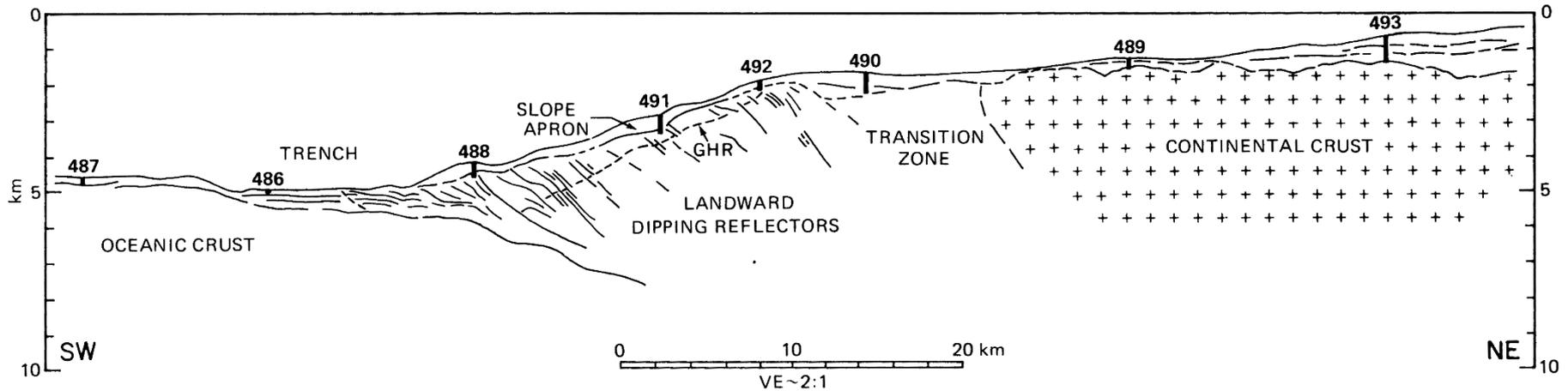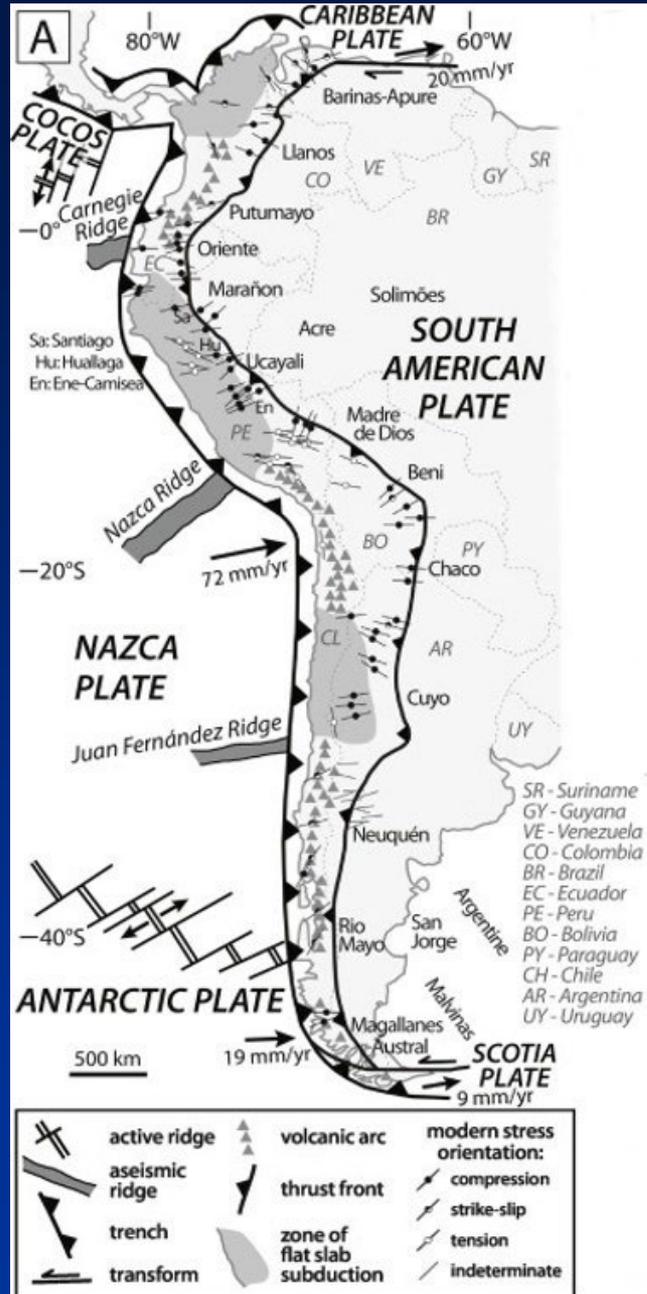
Prismi di accrezione

Figure 7. Cross section across the Middle America Trench off Southern Mexico in the Leg 66 drilling area (Moore and others, 1982). Vertical exaggeration (VE) is about 2:1.

Da Moore & Lundberg, 1986

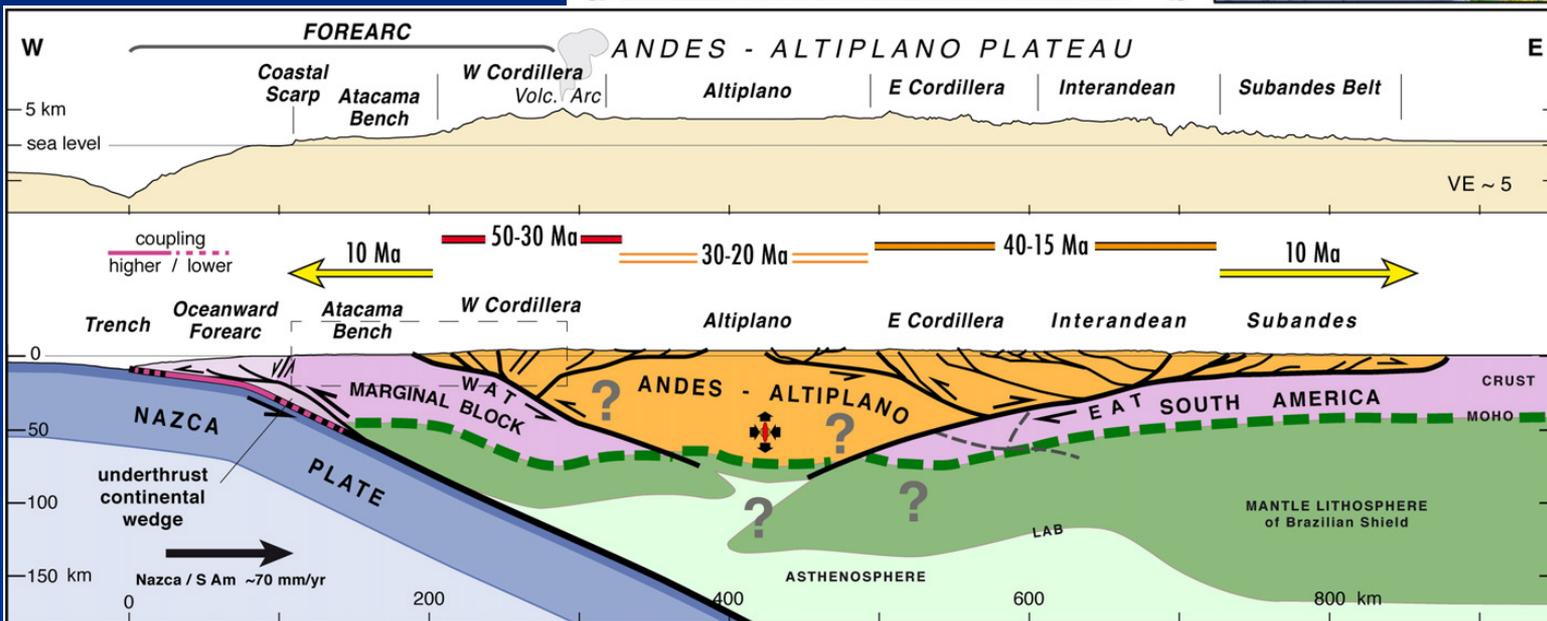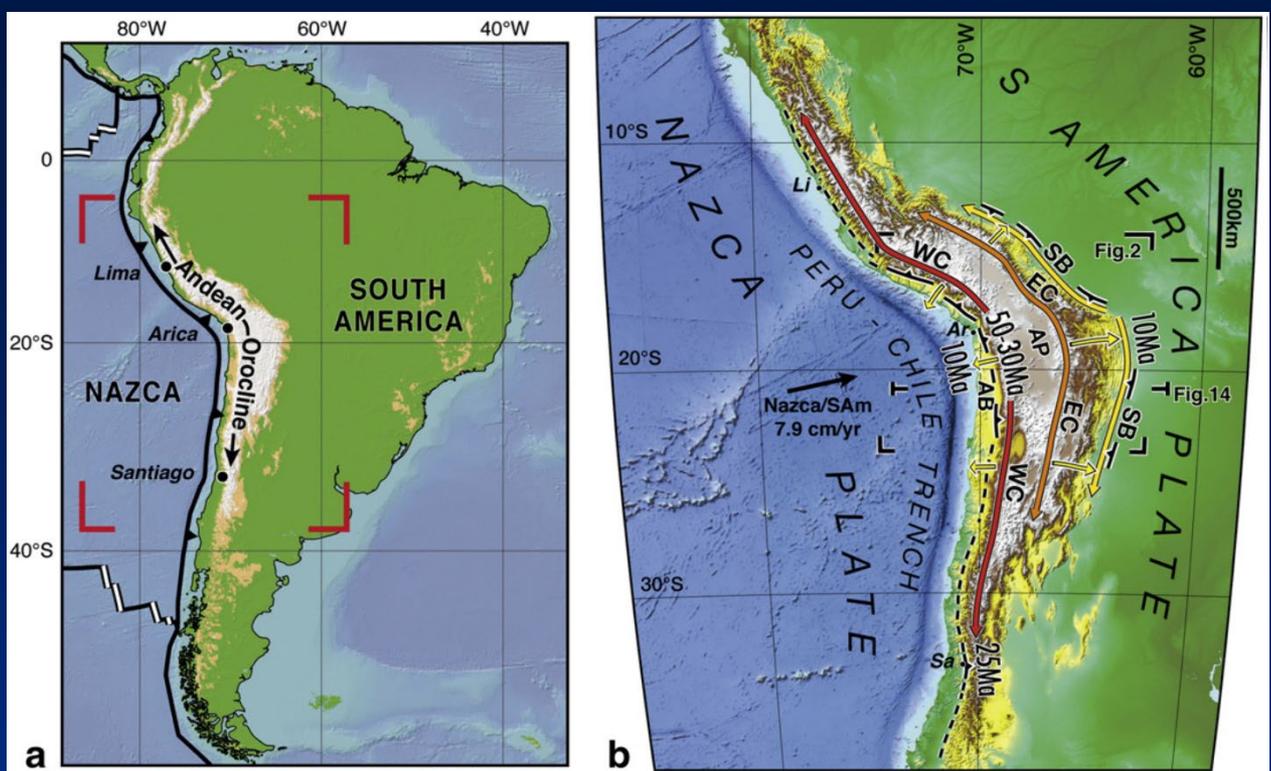Tipo cordillera o andino

https://commons.wikimedia.org/wiki/File:Tectonic_plates_boundaries_detailed-en.svg

Da Horton, 2018

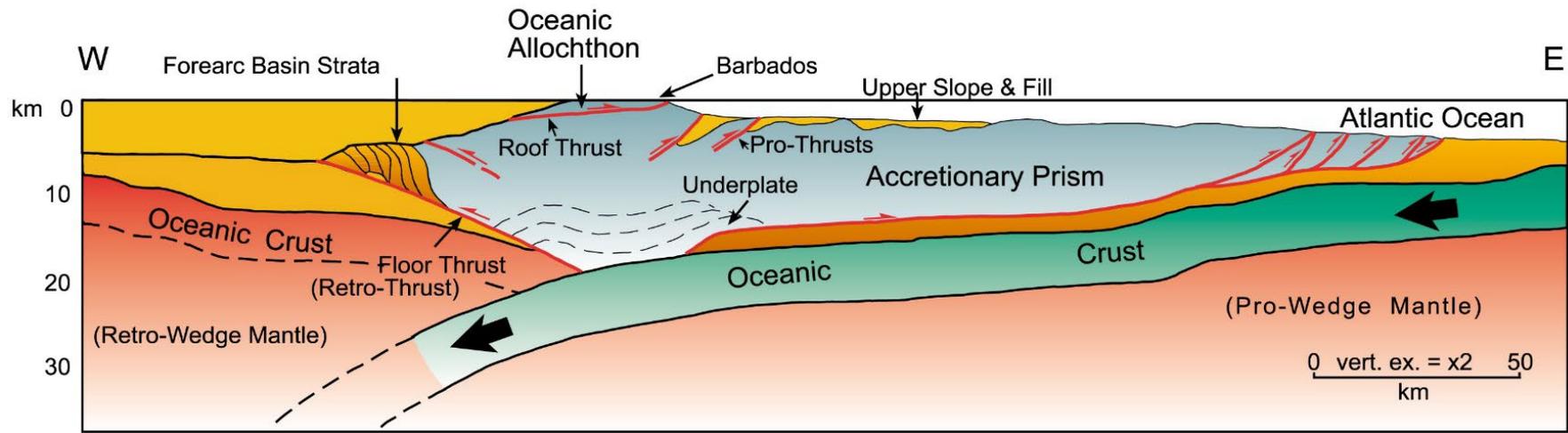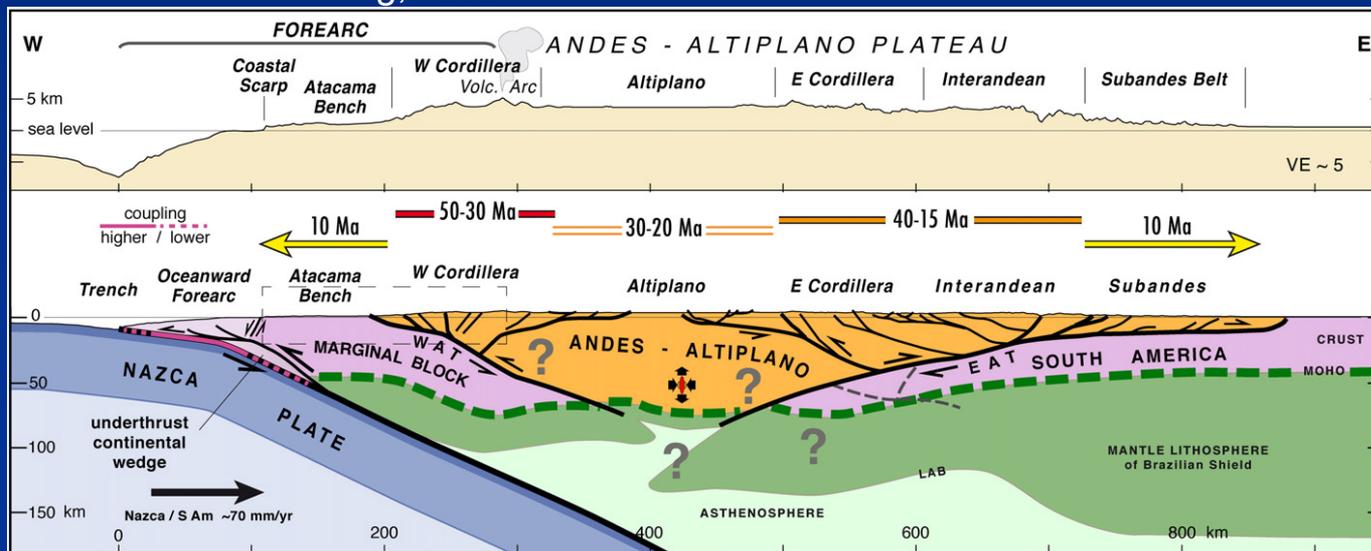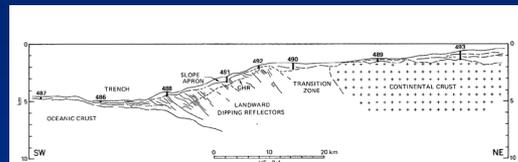Da Armijo et al., 2015

Da Armijo et al., 2015

Da Armijo et al., 2015; Moore and Lundberg, 1986

Prismi di accrezione: i due tipi
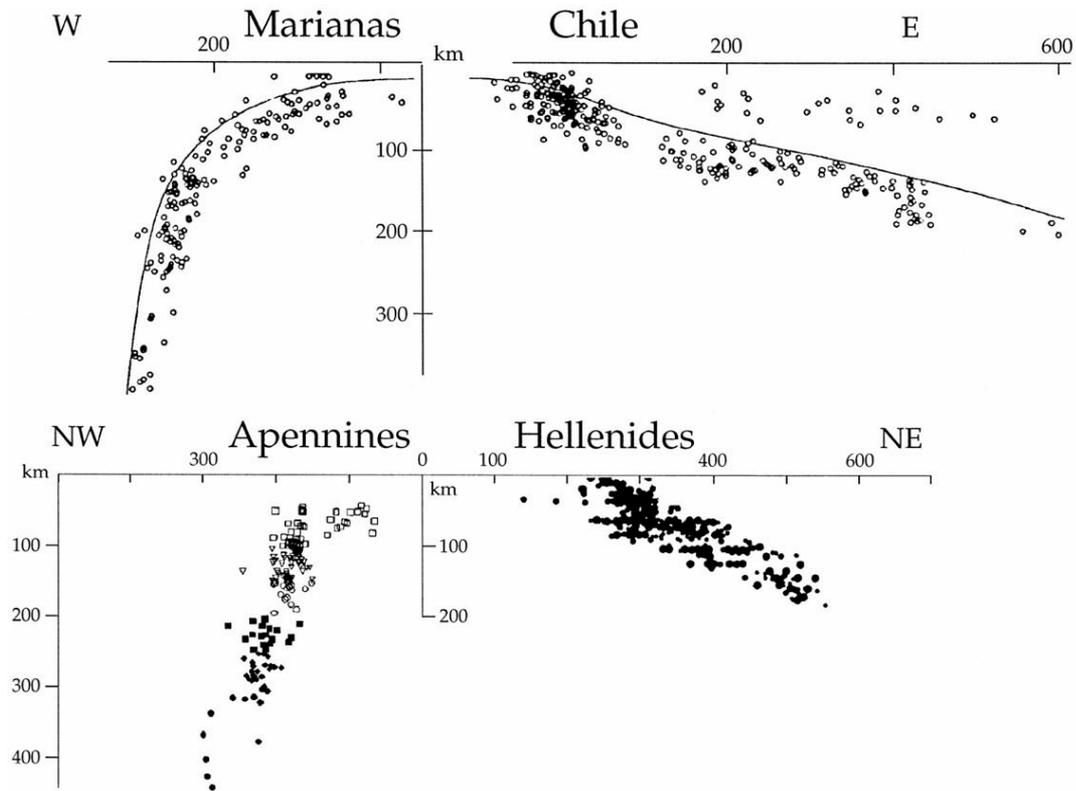
Fig. 3. Ipocenters of the Marianas and Chile subduction zones in the Pacific (after Isacks and Barazangi, 1977), compared with the seismicity of the Apennines (Selvaggi and Chiarabba, 1995) and Hellenides (Papazachos and Comninakis, 1977) opposed subduction zones. The Pacific asymmetry is present also in the central Mediterranean subduction zones where the Ionian oceanic lithosphere is subducting contemporaneously both underneath the Apennines and the Hellenides. Location of the sections in Fig. 2.

Da Doglioni et al., 1999

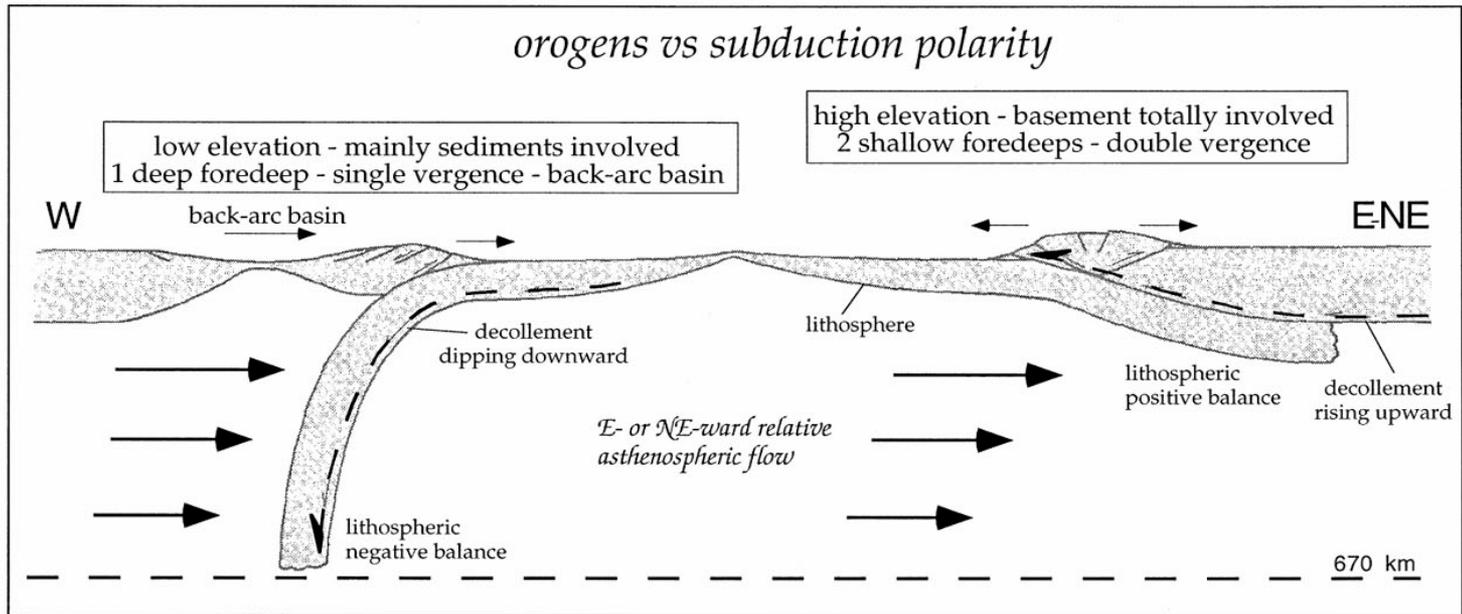Fig. 5. W-directed subduction zones are steeper and deeper with respect to the E–NE- or NNE-directed subduction zones. Note that the decollement plane of the eastern plate is warped and subducted in case of W-directed plane, whereas it ramps toward the surface in the E–NE-directed subduction, enabling the uplift of deep seated rocks: this asymmetry may be explained by the 'westward' drift of the lithosphere relative to the mantle and controls the strong differences in morphology, structure and lithology of the related thrust belts.

Da Doglioni et al., 1999

Active Back-Arc Basins (BAB) of the World
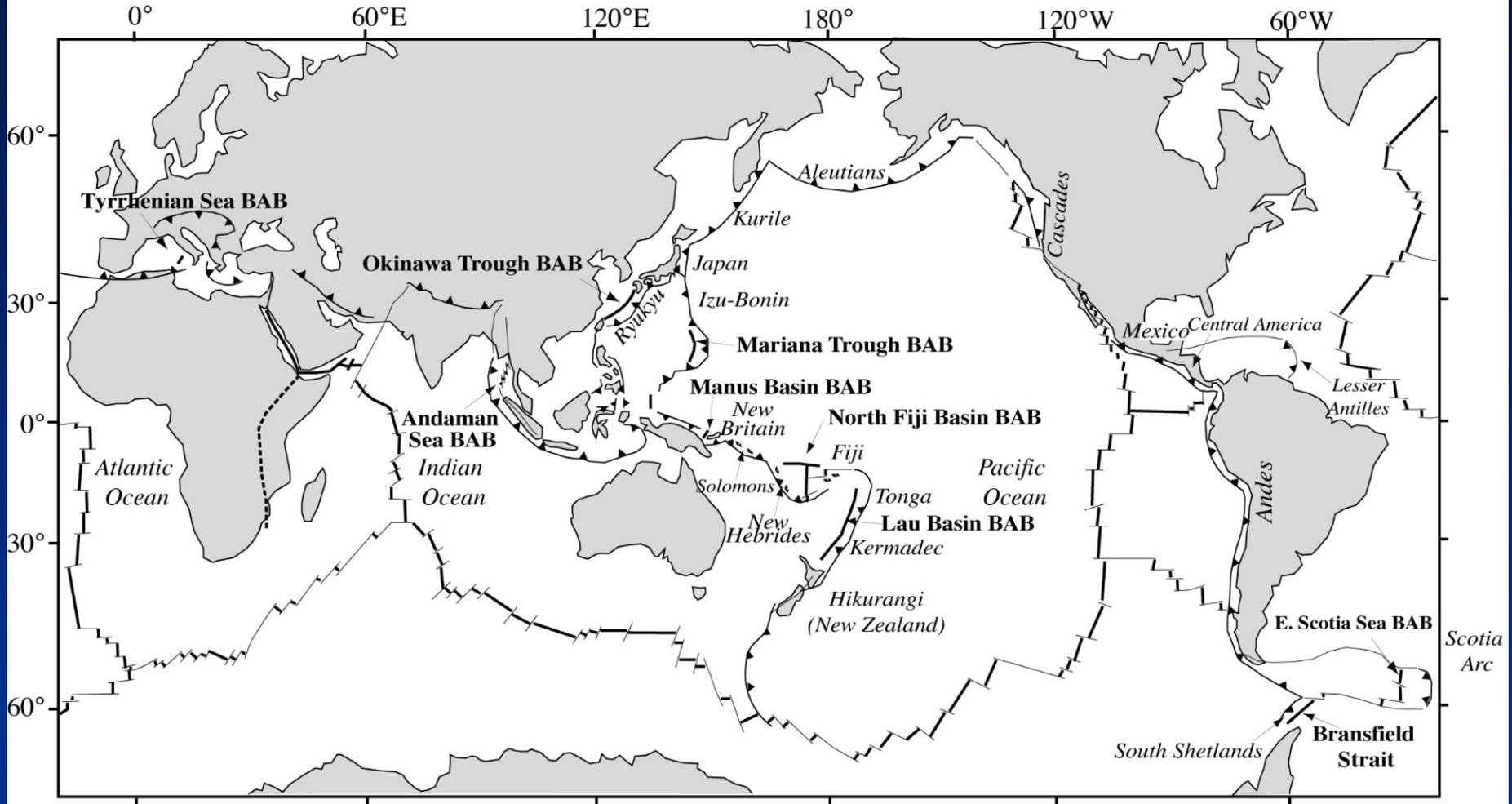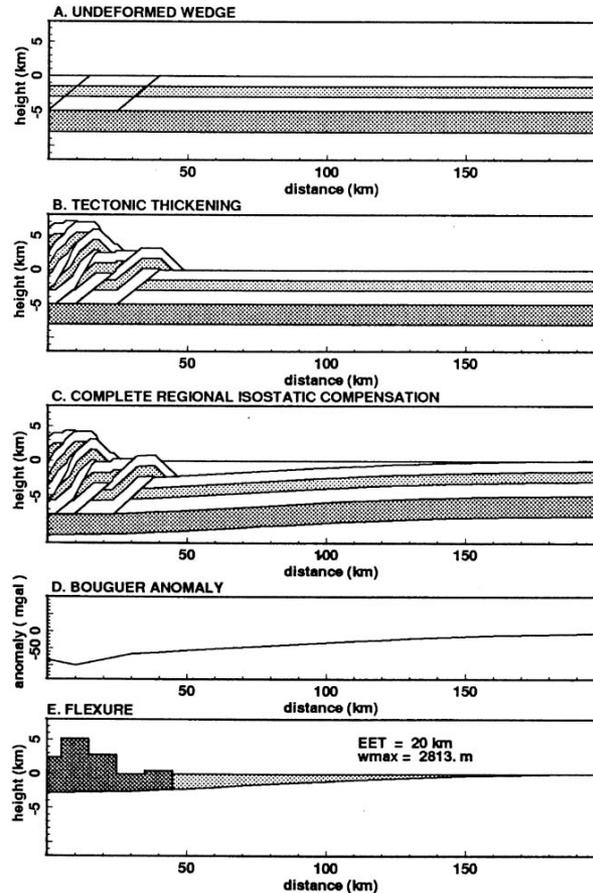
Foreland system: flessura della litosfera

Figure 2-1. Effect of thrust loading on lithospheric response. Regional isostasy results in depression filled with sediments, a) initial situation, b) emplacement of thrust sheets onto the craton, c) flexural response to thrust mass loading, d) associated Bouguer gravity anomaly, e) flexure in (c) calculated with thrust load and sediment load on lithosphere with 20 km effective elastic thickness (EET), quantified after Price [1973].
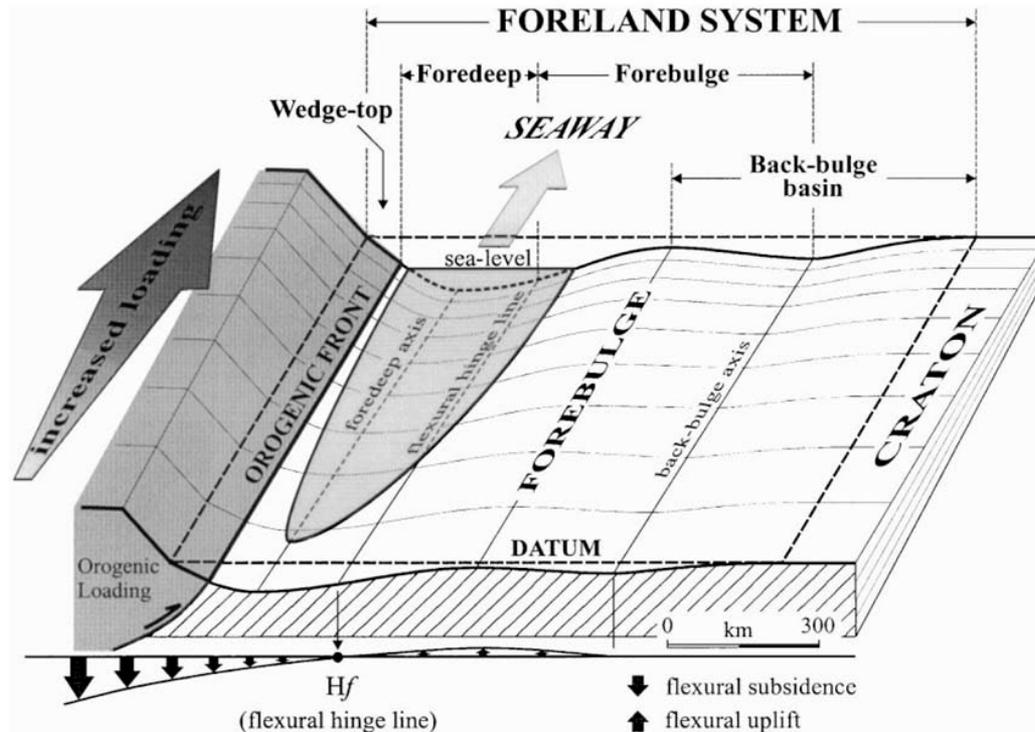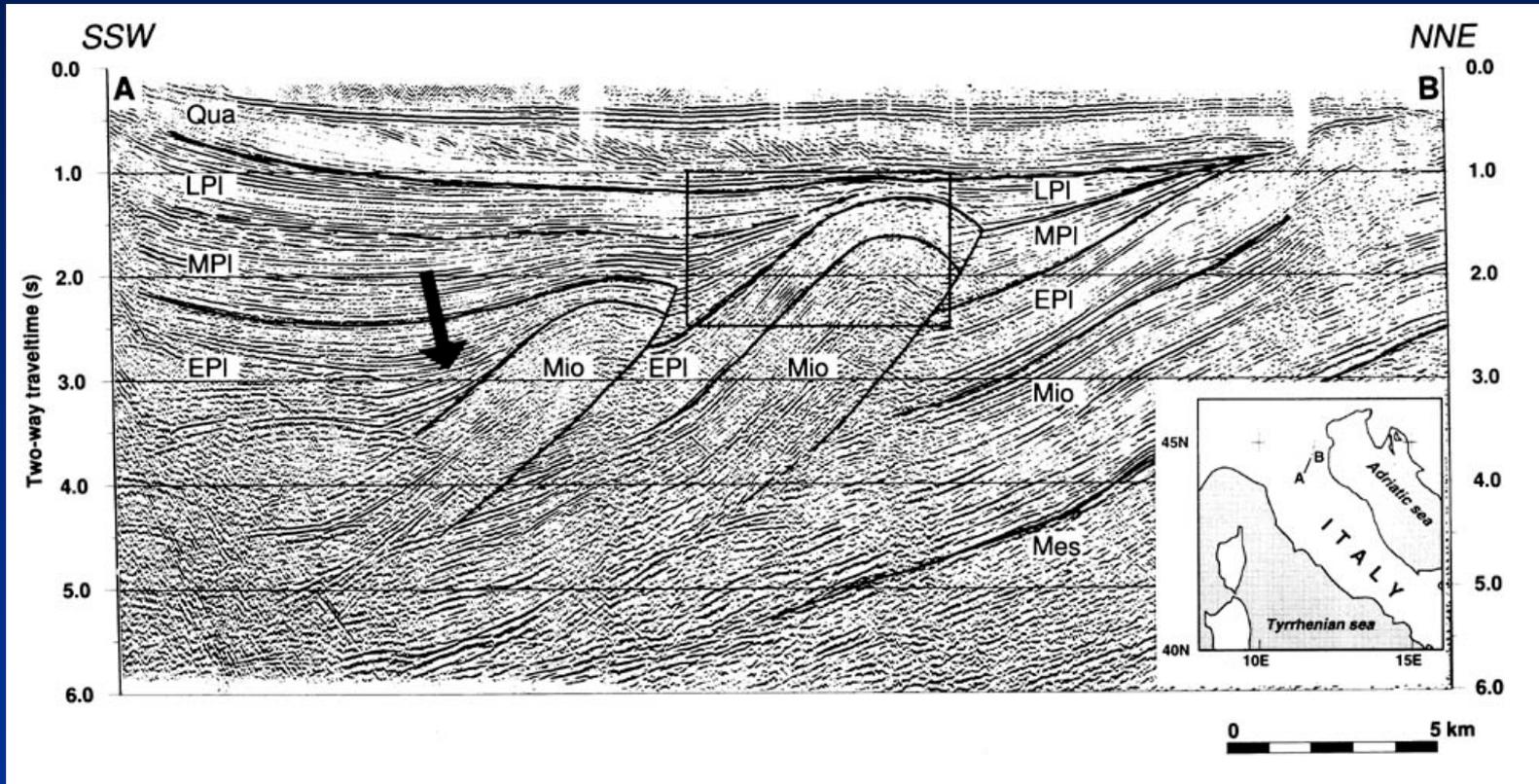
Da Zoetemeijer, 1993

Fig. 3. Configuration of the foreland system during orogenic loading with strike variability. The magnitude of the flexural deflection is proportional to the degree of loading. Four depozones may be differentiated, i.e. wedge-top, foredeep, forebulge and back-bulge. We refer to the wedge-top and foredeep as the proximal sector, and to the forebulge and back-bulge as the distal sector. The proximal and distal sectors of the foreland system are separated by the flexural hinge line. The topographic elevation of the adjacent craton, approximated with a horizontal plane, is taken as a datum. The base-level of deposition within the foreland system may be in any position (below, above or superimposed) relative to the datum, although surface processes on the craton (sedimentation, erosion) tend to adjust the datum to the base-level.

Da Catuneanu et al., 2000

Cunei sedimentari sin-tettonici: la Pianura padana
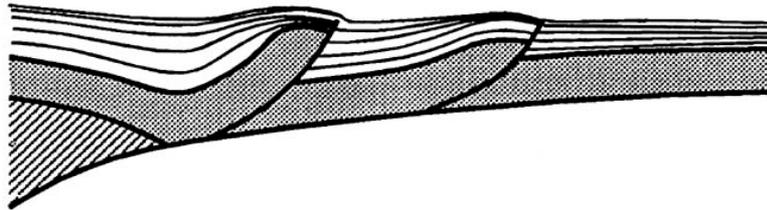

Da Zoetemeijer, 1993

A. pre-tectonic sedimentation
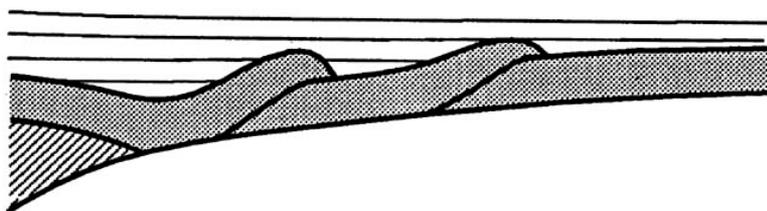
B. syn-tectonic sedimentation

Figure 4-2. Schematic representation of possible basin configurations with sediment deposition (a) before, (b) during, and (c) after thrust interference (modified from Ricci Lucchi, 1986).

C. post-tectonic sedimentation

Da Zoetemeijer, 1993